A Review on Rainfall Data Resolution and Its Role in the Hydrological Practice

Renato Morbidelli * , **Carla Saltalippi** , **Jacopo Dari** and **Alessia Flammini**

Department of Civil and Environmental Engineering, University of Perugia, Via G. Duranti 93,
06125 Perugia, Italy; carla.saltalippi@unipg.it (C.S.); jacopo.dari@unipg.it (J.D.); alessia.flammini@unipg.it (A.F.)
* Correspondence: renato.morbidelli@unipg.it; Tel.: +39-075-585-3620

Abstract: Data collected by gauges represent a fundamental force in most hydrological studies. On the basis of sensor type and recording system, such records are characterized by different aggregation time, t_a. In this review paper, a comprehensive rainfall database of rain gauge networks operative worldwide is used to determine the temporal evolution of t_a. As a second step, issues related to the limited and heterogeneous temporal resolution of rainfall data are discussed with regard to avoiding possible errors in the analysis of historical series. Particular attention is focused on quantifying the effects on the estimation of extreme rainfalls that play a crucial role in designing hydraulic structures. To this aim, algebraic relations for improving a correct determination of extreme rainfall are also provided.

1. Introduction

As is widely recognized, rainfall data is necessary for the mathematical modelling of extreme hydrological events, such as droughts or floods [1], as well as for evaluating surface and subsurface water resources and their quality.

The phase, quantity, and elevation of generic hydrometeors in the atmosphere [2–6] can be estimated by ground-based radars. Satellites can provide images with visible and infrared radiation, and they can also serve as platforms for radiometers to derive the quantity and phase of hydrometeors [7–14]. Radars and satellites provide spatial information on precipitation at wide scales, avoiding many problems connected to local ground measurements, including those for the areal inhomogeneity of a network [15]. However, direct rainfall observations at point scale can be obtained only by rain gauges installed at the soil surface.

Direct rainfall data can be automatically recorded or not. Typically, non-recording gauges are open receptacles with vertical sides, where the rainfall is derived by human observation on a graduated cylinder. Recording gauges automatically acquire precipitation depths at specified time steps and can be of different types: weighing, float, or tipping bucket gauges. A more recent device is the disdrometer, which can detect the size distribution and speed of falling hydrometeors. A weighing-type rain gauge records the weight of the receiving container and the accumulated rainfall with a spring mechanism or a system of balance weights. A float-type rain gauge consists of a chamber containing a float that rises vertically when the water level increases. A tipping-bucket-type rain gauge works by means of a two-bucket system. The exchanging motion of the tipping buckets generates a signal, corresponding to a rainfall depth equal to the ratio between the water volume that produces a tipping and the surface area of the collector. The signal is recorded, providing a very accurate measure of rainfall depth. In fact, most tipping bucket sensors are set up to obtain one signal for each 0.1 or 0.2 mm of rainfall.

When the direct local rainfall was recorded by means of human observation, a manual transcription of the total depth accumulated, typically in the previous 24 h, was performed. With the spread of automatic recordings, first on paper rolls (e.g., [16]) and later on digital supports, a higher temporal aggregation (or time resolution), t_a, of rainfall observation was achieved. Historical series of rainfall data are characterized by different t_a, due to the rain gauge type used, adopted recording system, and specific interests of the data owner.

From this historical background, it is clear that until the introduction of digital data loggers, rainfall data were characterized by coarse aggregation time, which may have influenced the results obtained by different kinds of analyses. As an example, several researchers evaluated the effect of coarse time resolution in estimating annual maximum rainfall depths, H_d, with fixed timescales, d [17–28]. All these studies showed that for d comparable with t_a, the actual values of H_d may be considerably underestimated by up to 50%. Thus, long series of H_d values typically include a relevant number of possible underestimated values deriving from rainfall data with coarse t_a, grouped with elements obtained from high-time-resolution data recorded in the last two to three decades. This issue, together with other crucial elements (relocation of stations, use of different rain gauge types, and change of station surroundings), may determine relevant effects on many related investigations, such as those related to the determination of rainfall depth–duration–frequency curves [28] and the evolution of extreme rainfall trends [29].

The problem of underestimated annual maximum rainfall depth could be solved for durations greater than 1 h by adopting one of the methodologies suggested by the scientific literature [17–28], while the same cannot be easily done for the analysis of heavy rainfalls characterized by sub-hourly durations. In fact, long H_d series for $d < 1$ h are rarely available for most geographical areas [29]. The number of rain gauges operative worldwide is approximately in the range 150,000–250,000 [30–34]. As networks of different geographical areas have specific histories and management objectives, the time resolution of the available rainfall data may differ.

The main objective of this review paper is to address the aforementioned issues, regardless of the equally important problem of measurement errors, to improve the use of historical extreme rainfall series through their homogenization with respect to t_a. Particular attention is reserved for the correction of H_d series, with the aim of avoiding distortions in climate change detection and hydraulic structures design.

Specifically, first, the history of the time resolution of rainfall records at the global scale is presented. Secondly, the length of H_d series required to estimate an average corrector factor is defined in order to reduce the original error of each series element characterized by a given temporal aggregation. Lastly, a methodological approach producing homogeneous series of H_d from data derived through different t_a is provided. Two additional issues of relevant interest are also investigated: the sensitivity of rainfall depth–duration–frequency curves to H_d corrections, and the effects of underestimated H_d values on trend analyses directed to check if climate change is affecting the intensities and frequencies of extreme rainfalls.

Finally, independently of the main objective of this paper, we note that well-known measurement errors (e.g., the amount of rainwater lost during the tipping movement of the bucket, wind influence on precipitation measurements due to interaction between the gauge body and the airflow, debris in the bucket, inappropriate location of the sensor) remain mostly ignored, and the historic information contained in the archived rainfall series continues to be affected by significant biases and uncertainties. Such errors propagate in the derivation of rainfall statistics related to the expected frequency of rainfall events, the calculation of design rainfall for engineering works, and other hydrological applications. The same is true in the field of climatology, where the quality and homogeneity of historic rainfall records is imperative to ensure that the assessment of possible climatic trends is correctly substantiated.

2. Rainfall Data Characteristics

Rainfall data available in several geographic areas are characterized by different temporal aggregation, mainly due to the specific network scope manager and to the technology of the devices used. At present, most rainfall data are continuously recorded in digital data loggers, allowing the adoption of any aggregation time interval, even equal to 1 min (Figure 1).

Figure 1. Rain gauge with digital data logger correctly working at Perugia (central Italy).

Until the 1990s, rainfall observations were recorded on paper rolls (see Figure 2) typically with t_a = 30 min or 1 h. In addition, before the Second World War, the time resolution of rainfall was daily, with manual recording once a day at a fixed time (see Figure 3).
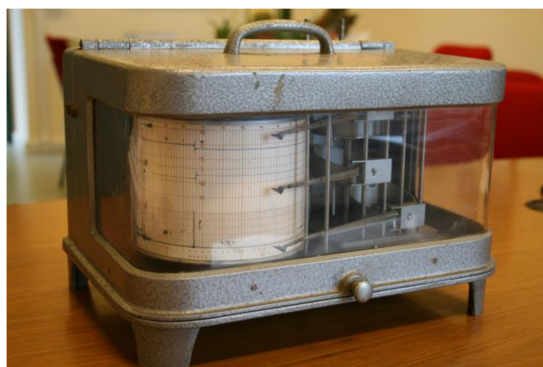

Figure 2. A typical mechanical recorder with paper rolls.

OSSERVAZIONI PLUVIOMETRICHE GIORNALIERE

BACINI PRINCIPALI E STAZIONI	Tipo dell'apparecchio	ALTEZZE DI PRECIPITAZIONE IN MILLIMETRI D'ACQUA OSSER																		
		1	2	3	4	5	6	7	8	9	10	11	12	13	14	15	16	17	18	19	20
Fossato di Vico	Pn	—	—	—	—	5.0*	4.0*	—	—	—	—	—	4.3*	—	—	20.2*	10.0*	—	—	—	—
Costacciaro	Pn	—	—	—	8.0*	—	—	—	—	7.0*	—	—	—	—	—	6.0	—	—	—	—	3.0
Gubbio	Pn	—	—	—	12.0*	6.6*	—	—	0.2*	—	—	—	—	7.0*	—	—	10.0	6.0	—	—	—
Padule	P	—	—	—	—	8.5*	0.9*	—	0.5*	—	—	—	—	7.3*	—	—	5.5	3.0	—	—	—
Pieve di Compresseto	Pn	—	—	—	19.9*	1.2*	—	—	0.8*	—	—	—	1.9	10.0	—	—	11.3*	1.1	—	—	—
Gualdo Tadino	P Pr	—	—	0.8	20.0	7.5	0.5	—	1.0	1.0	5.0	—	—	—	—	—	3.5	0.5	—	—	—
Valfabbrica	P	—	—	7.0	20.2*	8.0*	1.0*	3.0*	—	—	—	10.0	3.0	—	—	—	10.0	12.0	—	—	—
Pianello	P	—	—	—	27.2*	—	—	—	—	—	—	—	3.5	4.7	—	0.1	10.6	1.1	—	—	—
Assisi	P	—	—	—	10.0	10.0	—	—	—	—	—	—	—	—	—	—	27.0	—	—	—	—
Bastia	P	—	0.2	—	31.5	0.3	—	—	—	—	0.5	—	0.3	3.3	0.2	1.1	13.7	1.2	—	—	—
Bagnara	Pn	—	—	—	19.0	27.0*	—	—	—	—	—	—	—	9.8*	—	—	13.4	3.5	—	—	—
Nocera Umbra	Pn	—	—	9.0*	—	—	—	—	—	—	—	—	—	5.0	—	—	4.0	3.2	—	—	—
Annifo	Pn	—	—	—	2.0	65.0*	—	—	—	—	—	—	—	12.0	22.0*	10.0	8.0	—	—	—	—
Rasiglia	Pn	—	—	—	38.0*	7.0*	—	—	—	—	—	1.0	—	25.0*	—	—	15.0*	—	—	—	—
Valtopina	Pn	—	—	25.0*	15.0*	—	—	—	—	—	—	—	—	13.0	—	—	11.5	8.0	—	—	—
Foligno	P	—	—	19.0	—	—	—	—	—	—	—	14.0	8.0	—	—	12.0	8.0	1.0	—	—	—
Mogliano	P	—	—	—	27.0	6.3*	—	—	—	—	—	—	9.8	—	—	8.3	4.0	—	—	—	—

Figure 3. Transcription of manual recording of daily rainfall data during two decades of January 1922 for some rain gauge stations located in central Italy.

3. Rainfall Data Time Resolution at Global Scale

A database with information about the time resolution of rainfall data in different geographic areas of the world was recently published [35]. It provides, for each of the 25,423 rain gauge stations considered from 32 study areas, the complete t_a history and the site geographical coordinates (see Figure 4). The main characteristics of the available rainfall observations, grouped by continent, are shown in Table 1.

As is deducible from Table 1, the collected stations are not evenly distributed around the world, but they can be considered a good sample of different monitoring records that can be found in the world (for details see [35]). In a limited number of study areas considered in [35], the length of rainfall data series with known t_a is close to 200 years (see Figure 5), while in most areas it is about 100 years. In addition, in a few cases, the t_a history is available for recently installed stations.
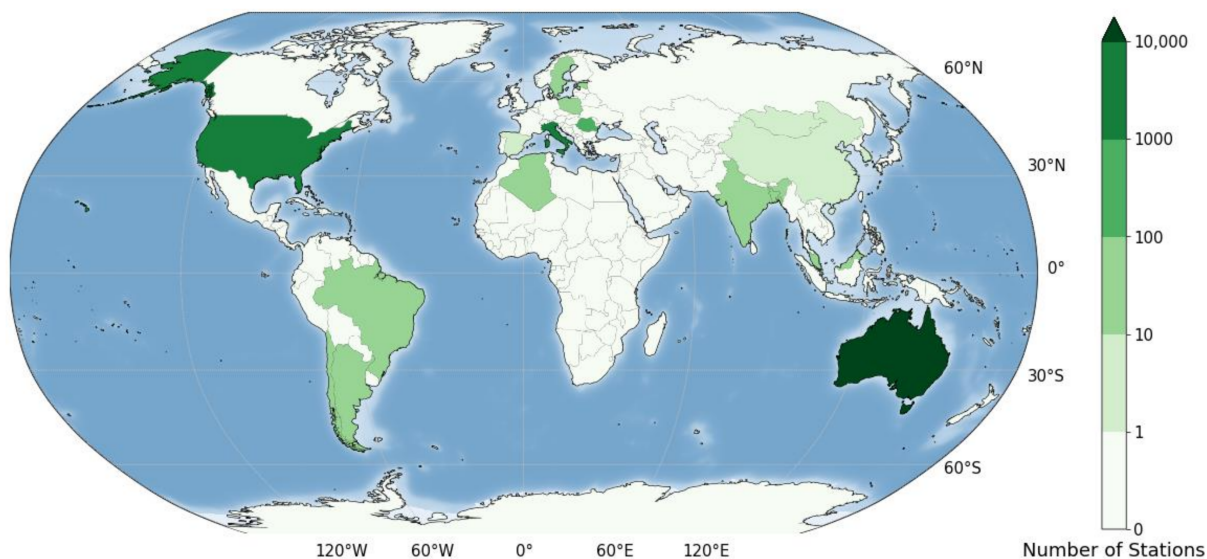
Figure 4. Geographical position of the rain gauge stations considered by Reference [35].

Table 1. Main characteristics of the available rainfall recordings for the rain gauge stations included in the database set up by Reference [35] grouped by continent.

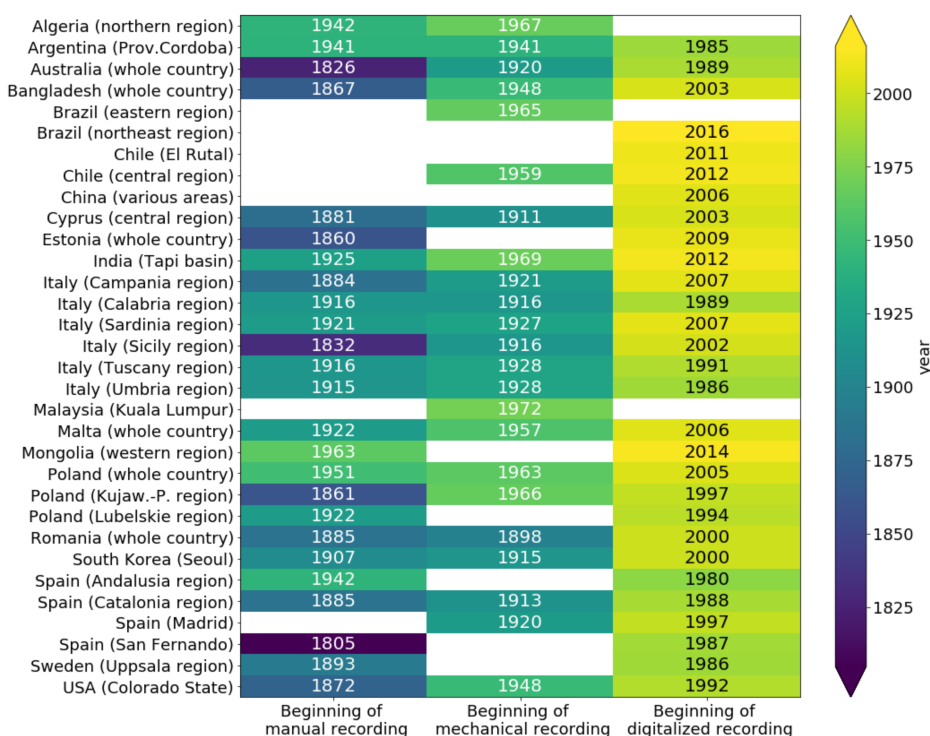| Continent	Rain Gauges (Number)	Record Length min/max (Years)	Beginning of Records (Year)	Ending of Records (Year)	Time Resolution min/max (Minutes)
Africa	30	9/41	1968	2010	1440
America	5779	1/153	1867	2019	1/1440
Asia	148	5/112	1879	2019	1/1440
Australia	17,768	1/180	1805	2019	1/1440
Europe	1642	1/184	1805	2019	1/43,200

Figure 5. Year of beginning of manual, mechanical, and digital rainfall recordings for the study areas considered in [35].

In many study areas, especially in cases of very old rain gauge stations, recording started by human observation (Figure 5) with coarse time resolution—typically of 1 day but sometimes of 1 month or 1 year. The oldest rainfall data recorded in manual mode (San Fernando station, Spain, since 1805) exhibits t_a equal to several days.

Except for a few cases, mechanical recording on paper rolls started in the first decades of the 20th century. For instance, mechanical recordings with t_a = 60 min have been carried out at Alghero station (Sardinia region, Italy) since 1927 and at Campulung station (Romania) since 1949.

The introduction of digital data logging took place in the last decades of the 20th century. As a consequence, the investigations of climate change effects on short-duration (sub-hourly) heavy rainfalls are unreliable in almost all geographic areas due to the shortness of rainfall series. Currently, through tipping-bucket sensors, rainfall amounts are recorded in data loggers for each tip time associated with a fixed rainfall depth (0.1 or 0.2 mm). Then, rainfall data can be aggregated with any t_a (also equal to 1 min). Borgo S. Lorenzo station (Tuscany region, Italy) and Valletta station (Malta) are two examples of digital data characterized by t_a = 1 min recording since 1991 and 2006, respectively. Exceptionally long series of high-resolution rainfall (e.g., Malaysia) were taken out by automatic systems from strip charts of tipping-bucket gauges [16].

Due to the heterogeneity of the database stations, it is hard to synthesize by unique figures and tables the history of all the study areas considered in [35]. In some countries, the history of a single rain gauge is available, as in the case of the Madrid station, while in some others, a network with thousands of rain gauges is involved, as in the case of Australia and Colorado (United States). In any case, Figure 6 attempts to solve the problem by showing the percentage of rain gauges with specific t_a for all the stations except those of Australia and Colorado (United States), whose huge numbers would make the plot confusing. From Figure 6, it is possible to deduce that about 50% of stations today have adopted $t_a = 1$ min due to the spread of continuous recording, while data with $t_a = 1440$ min are going to disappear in the near future.
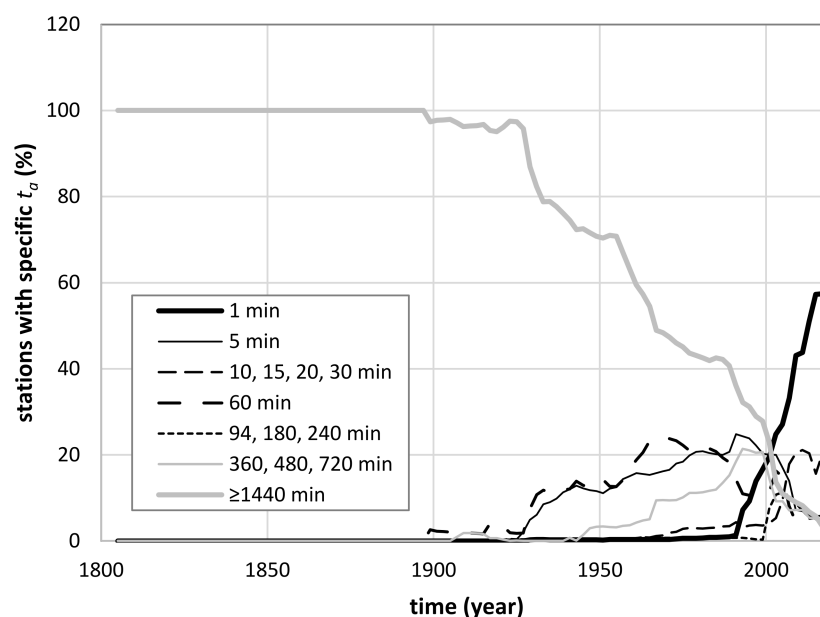

Figure 6. Percentage of rain gauge stations with specific temporal aggregation, t_a, as a function of time. All the stations included in the analysis by Reference [35], except those located in Australia and Colorado (United States), are considered.

By the analysis of [35], it is evident that the registration methods of the rain gauge stations changed over time, passing first from daily manual recordings to mechanical recorders with t_a equal to 30 min or 1 h, and then to continuous recording with digital data loggers. The changes from one recording type to another were not simultaneous, as both Figures 5 and 6 show.

4. Effect of Rainfall Time Resolution on Estimating Annual Maximum Depths

Errors in the estimates of extreme rainfalls due to different values of d for a specific t_a have been widely investigated in the scientific literature. Specifically, it has been shown that for d close to t_a, the actual maximum rainfall depth may be underestimated [17–28]. Some useful approaches have been published to adjust for this underestimation. For example, Reference [18] observed that for $d = t_a$ the results obtained from an analysis based on actual maxima were closely approximated through a frequency analysis of H_d with values multiplied by 1.13. Reference [19], using a probabilistic methodology under the hypothesis of a constant rainfall over the duration of interest, provided a relationship between the sampling ratio, t_a/d, and a sampling adjustment factor (SAF). This last quantity is defined as the average ratio of the real maximum rainfall depth for a given d to the maximum one deduced by a fixed recording interval. Reference [25], on the basis of high-temporal-resolution data from 15 rain gauges located in the Kansas City metropolitan area, proposed an empirical relationship between SAF and sampling ratio that provided corrections coherent with other experimental studies (e.g., [36]). However, the limited

length of the available rainfall series (in the range 5.3–14.9 years, with average value of 9.6 years) made it impossible to obtain general conclusions. Reference [26] extended the probabilistic methodology used in [19] to temporally variable rainfall distributions and found it to be significantly related to the SAF. A procedure to produce quasi-homogeneous annual maximum rainfall series involving data derived from different time resolutions was recently presented [28]. The authors proposed an algebraic relation that expresses the average underestimation error with the ratio t_a/d useful to correct the H_d values. All the aforementioned investigations show that the SAF depends on the sampling ratio as well as on d because the duration influences the shape of the rainfall's temporal distribution.

4.1. Hyetograph Shape and H_d Underestimation

Following [37,38], indicating by $x(t)$ the rainfall depth observed at time t at a specific site, the cumulative rainfall recorded over a time period d, $x_d(t)$, is expressed as:

$$x_d(t) = \int_t^{t+d} x(\xi)d\xi \tag{1}$$

and the annual maximum rainfall depth over a duration d is given by:

$$H_d = max[x_d(t) : t_0 < t < t_0 - d + 1year] \tag{2}$$

where t_0 is the starting time of each year.

To estimate H_d for each year, the availability of rainfall observations with $t_a \leq d$ is necessary. When $d = t_a$, independently of the rainfall distribution shape, the H_d value can be correctly estimated (Figure 7a) or underestimated (Figure 7b,c) with errors up to 50%.
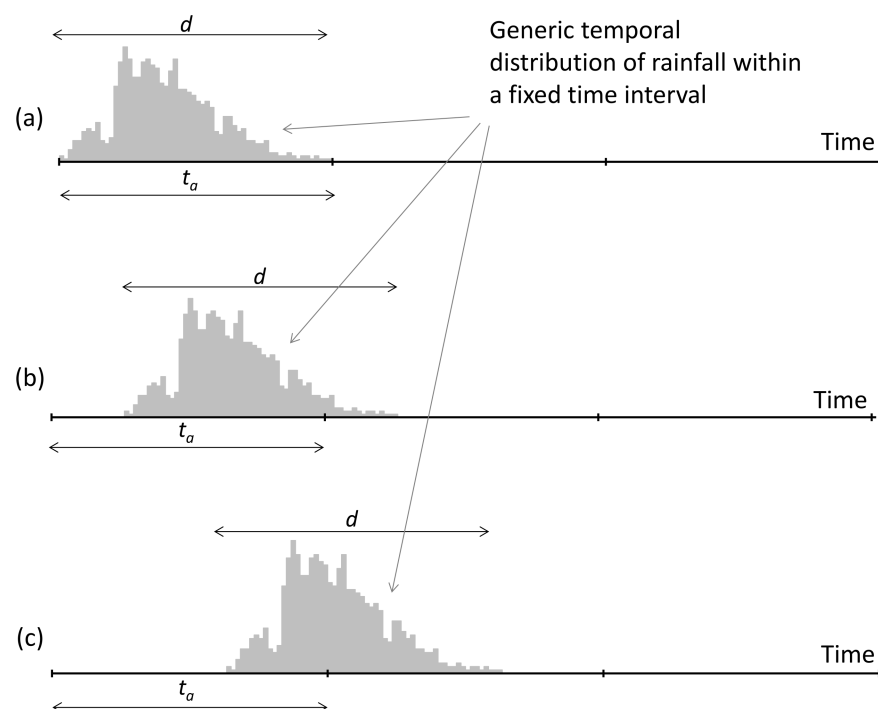

Figure 7. Schematic representation of a generic temporal distribution of rainfall with duration $d = t_a$: (**a**) condition where a correct evaluation of H_d is possible; (**b**) condition with a generic underestimate of H_d; (**c**) condition with the maximum underestimate of H_d (equal to 50%). t_a and H_d denote the temporal aggregation and annual maximum rainfall rate of duration d, respectively.

A quantification of the accuracy of a given H_d value is not available, but it is possible to represent the average error for a temporal series with a large number of elements.

For each duration d, this average error depends on both t_a and the shape of the rainfall hyetographs. In the case of rectangular shapes, the average underestimate is equal to 25%, because each error value in the range 0–50% has the same probability of occurrence. This result is in accordance with the analysis by [26]. However, as is widely recognized, the H_d values typically belong to heavy rainfalls of erratic shape [39–41].

For example, under the hypothesis of a triangular rainfall shape with duration d, the total rainfall depth, R_{pd}, is:

$$R_{pd} = \frac{dh}{2} \tag{3}$$

with h equal to the rainfall intensity peak.

In case of $t_a = d$, the underestimation error of a single H_d is still in the range 0–50%, but the associated average value, E_a, derived by integrating through the rainfall duration (see also [26]) becomes:

$$E_a = \frac{1}{12} t_a h \tag{4}$$

This quantity, expressed in terms of rainfall depth percentage, is expressed as:

$$E_{a\%} = 100 \frac{E_a}{R_{pd}} \tag{5}$$

such that for $t_a = d$ is equal to 16.67%, in accordance with the results in [26].

Experimental evidence from different rain gauge stations and d values indicate a steeper trend of rainfall before and after the peak; thus, the actual values of $E_{a\%}$ should assume values lower than 16.67%.

In any case, independently of the adopted t_a, underestimation errors in determining the H_d values cannot be eliminated. The average error $E_{a\%}$ decreases if the ratio t_a/d decreases. Specifically, from Equations (3) and (5), it can be expressed as:

$$E_{a\%}(d = nt_a) = \frac{1}{n} E_{a\%}(d = t_a) n = 1, 2, \ldots \tag{6}$$

becoming negligible for sufficiently small t_a/d.

On this basis, for $d = t_a = 1$ min, in the case of an extreme rainfall with rate of 300 mm/h, the underestimation error is lower than 1 mm. In addition, as the durations of interest for H_d are generally ≥ 5 min, rainfall observations with $t_a = 1$ min may be considered to have negligible error.

4.2. Correction Procedure for H_d Series

When rainfall records are characterized by coarse time resolution, the underestimation error in the determination of the annual maximum rainfall depth for a fixed d can be considered as a random variable following an exponential probability distribution with entity inversely correlated to H_d [42]. Correction through the use of the average error has relevant effects only if it involves a large number of underestimated values. For example, Reference [28] proposed a lower limit of 15–20 years for the series length to obtain a reliable estimate of the average error, especially when $d \approx t_a$, because for shorter series the error exhibits an irregular trend. The last outcome is in contrast with the analysis by Young and McEnroe [25], who considered rainfall depth series of about 10 years in length.

An overall analysis of the available studies suggests that:

- On a specific value, the underestimation error has a random behaviour and is within 50%;
- The average error depends on both t_a/d and d;
- The average error can be approximately supposed independent from the device location;
- The largest value of the average error occurs for $d = t_a$ and is theoretically less than or equal to 16.67%;

-      In the case of $d = nt_a$, the average error is less than or equal to $(1/n) \times 16.67\%$.

The aforementioned error considers the effect of time resolution on H_d values, either for a single year or for historical series. The described procedure allows for an increase in the homogeneity of H_d data series deriving from rainfall observations characterized by very different temporal aggregations.

Figure 8 shows the relationships proposed in [19,25,28] to quantify the average underestimation with variable ratio t_a/d. Reference [19] originally proposed the function expressed as:

$$E_{a\%} = 12.501\frac{t_a}{d} \ (\%) \tag{7}$$

and considered a probabilistic approach assuming a constant rainfall rate through the duration, while Young and McEnroe [25], by using H_d observed series, derived the following relation:

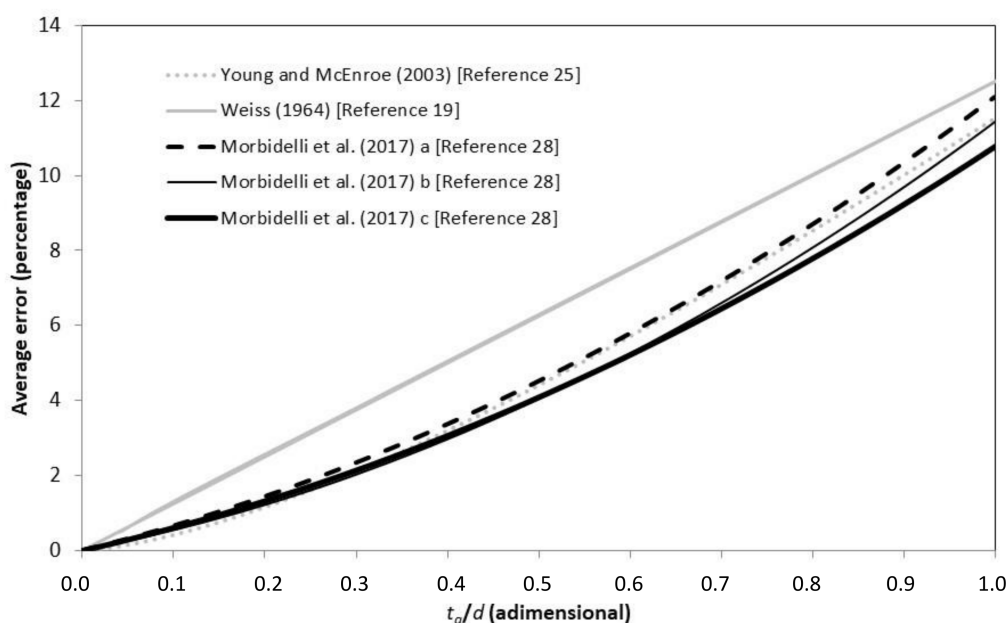$$E_{a\%} = 100 - \frac{100}{1 + 0.13\left(\frac{t_a}{d}\right)^{1.5}} \ (\%) \tag{8}$$

Figure 8. Average underestimation error of the annual maximum rainfall depth for different values of the ratio between time resolution, t_a, and duration, d, obtained by Equation (7) [19], Equation (8) [25], and Equations (9)–(11) [28]. In this last case, symbols "a", "b", and "c" stand for $d \leq 30$ min, d in the interval between 30 and 180 min, and $d \geq 180$ min, respectively.

Lastly, on the basis of the relationship between d and the rainfall shape that affects the error entity [26], Reference [28] proposed the following relations:

$$E_{a\%} = 6.14\left(\frac{t_a}{d}\right)^2 + 5.69\frac{t_a}{d} \ (\%) \ d \ \leq \ 30 \text{ min} \tag{9}$$

$$E_{a\%} = 6.7\left(\frac{t_a}{d}\right)^2 + 4.72\frac{t_a}{d} \ (\%) \ 30 \text{ min} \ < \ d \ < \ 180 \text{ min} \tag{10}$$

$$E_{a\%} = 5.2\left(\frac{t_a}{d}\right)^2 + 5.57\frac{t_a}{d} \ (\%) \qquad d \geq \ 180 \text{ min} \tag{11}$$

Relations (9–11) make it possible to correct the H_d series derived from data with coarse t_a as a function of d and t_a/d.

In principle, the relations by Reference [28] should be more effective because they make it possible to also consider the shape of the temporal distribution of rainfall in determining the correction factor. Along this line, Figure 8 shows that the equation from Reference [19] mainly produces larger average errors for intermediate values of the ratio t_a/d. On the contrary, the equation of Young and McEnroe [25], although also calibrated with very short data series, provides results comparable to those of Reference [28].

5. Role of t_a in Hydrological Applications

The observed heterogeneity in the t_a characteristic as a function of the considered geographic zone and epoch can affect further analyses based on H_d values, such as the determination of intensity–duration–frequency curves.

Specifically, the usage of long H_d series with underestimated elements for the determination of rainfall depth–duration–frequency curves produces errors of variable magnitude (up to 10%) with different return periods and rainfall duration [28]. These errors become relevant when the H_d series contain elements derived from a temporal aggregation much greater than 1 min. In addition, when designing hydraulic structures or restructuring existing ones, the effects on heavy rainfalls produced by climate change have to be considered, taking into account possible distortions due to the above errors in the H_d series.

In this context, [29] highlighted that the coarse time resolution of rainfall observations can substantially influence the results of widely used statistical techniques applied to check the possible effects of climate change on extreme rainfalls, such as, e.g., the least-square linear approach, the Mann–Kendall test, the Spearman test, and Sen's method. The following major insights were derived:

- Underestimation errors caused by coarse time resolution produce significant effects on least-squares linear trend analysis. The usage of a correction factor for the H_d values, independent of the selected approach, can make the trend sign change from positive to negative, and the effects are more evident for series with larger numbers of elements with $t_a/d = 1$.
- The non-parametric Mann–Kendall test [43,44] and the Spearman rank correlation test [45], with significance level equal to 0.05, exhibit a negligible sensitivity to underestimation errors on the H_d values.
- The application of Sen's method [46] gives different outcomes depending on whether uncorrected or corrected H_d values are considered.
- Because analysis of possible climatic trends requires data series at least 60 years long to include the effect of large-scale climate oscillations (see also [47]), it is not feasible to consider only rainfall data with $t_a = 1$ min that have historical series of only two/three decades in most geographic zones (see also [35]).
- Common homogeneity tests such as the standard normal homogeneity test for a single break point [48] or the Pettitt test [49] are not capable of detecting discontinuities in H_d series determined by different time resolutions. This result can be justified with the hypothesis that for annual maximum rainfall data, underestimation errors do not produce sufficiently relevant break points.

6. Conclusions

Rainfall observations are available with different time resolutions, with typical values between 1 min and 1 day, due to the development of recording systems over time. This review paper firstly analyses the history of t_a on the basis of a database that collects information on rain gauge networks working in many geographic areas of the world. The data collection illustrates that the rain gauge networks installed in the 19th century or at the beginning of the 20th century began recording in manual mode with coarse time resolution (from 1 day to 1 month), while mechanical recordings on paper rolls, with t_a typically in the range 30 min–1 h, were introduced in the first half of the 20th century. Digital data loggers were installed at the end of the 20th century, allowing any temporal aggregation (up to 1 min). At present, about 50% of stations have these characteristics. Many historical

rain gauge networks changed their registration systems over time, sometimes more than once, from manual to mechanical and lastly to digital.

This paper also shows that, due to the coarse time resolution of rainfall data, the use of series of "uncorrected" H_d values in determining rainfall depth–duration–frequency curves can lead to underestimates of about 10%. In addition, it can affect the results of the most common techniques applied to check climatic trends in extreme rainfalls. It is important to note that there are other sources of error (e.g., the amount of rainwater that is lost during the tipping movement of the bucket, wind influence on precipitation measurements due to interaction between the gauge body and the airflow, debris in the bucket, inappropriate location of the sensor) that can produce a wider distortion in the results.

By using specific algebraic relations between the average underestimation error and the ratio t_a/d, each H_d value can be adjusted, obtaining homogeneous H_d series that are usable for every kind of analysis.

References

1. Wilhelm, B.; Ballesteros Canovas, J.A.; Macdonald, N.; Toonen, W.; Baker, V.; Barriendos, M.; Benito, G.; Brauer, A.; Corella Aznar, J.P.; Denniston, R.; et al. Interpreting historical, botanical, and geological evidence to aid preparations for future floods. *WIREs Water* **2019**, *6*, e1318. [CrossRef]
2. Wilson, J.W.; Brandes, E.A. Radar measurement of rainfall. *Bull. Am. Meteorol. Soc.* **1979**, *60*, 1048–1058. [CrossRef]
3. Austin, P.M. Relation between measured radar reflectivity and surface rainfall. *Mon. Weather Rev.* **1987**, *115*, 1053–1070. [CrossRef]
4. Fread, D.L.; Shedd, R.C.; Smith, G.F.; Farnsworth, R.; Hoffeditz, C.N.; Wenzel, L.A.; Wiele, S.M.; Smith, J.A.; Day, G.N. Modernization in the National Weather Service River and Flood Program. *Weather Forecast.* **1995**, *10*, 477–484. [CrossRef]
5. Smith, J.A.; Seo, D.-J.; Baeck, M.L.; Hudlow, M.D. An intercomparison study of NEXRAD precipitation estimates. *Water Resour. Res.* **1996**, *32*, 2035–2045. [CrossRef]
6. Seo, D.-J. Real-time estimation of rainfall fields using radar rainfall and rain gage data. *J. Hydrol.* **1998**, *208*, 37–52. [CrossRef]
7. Barrett, E.C.; Beaumont, M.J. Satellite rainfall monitoring: An overview. *Remote Sens. Rev.* **1994**, *11*, 23–48. [CrossRef]
8. Sorooshian, S.; Hsu, K.-L.; Gao, X.; Gupta, H.V.; Imam, B.; Braithwaite, D. Evaluation of PERSIANN system satellite-based estimates of tropical rainfall. *Bull. Am. Meteorol. Soc.* **2000**, *81*, 2035–2046. [CrossRef]
9. Kuligowski, R.J. A self-calibrating real-time GOES rainfall algorithm for short-term rainfall estimates. *J. Hydrometeorol.* **2002**, *3*, 112–130. [CrossRef]
10. Turk, F.J.; Miller, S.D. Toward improved characterization of remotely sensed precipitation regimes with MODIS/AMSR-E blended data techniques. *Geosci. Remote Sens.* **2005**, *43*, 1059–1069. [CrossRef]
11. Joyce, R.J.; Xie, P.; Janowiak, J.E. Kalman filter-based CMORPH. *J Hydrometeorol.* **2011**, *12*, 1547–1563. [CrossRef]
12. Kucera, P.A.; Ebert, E.E.; Turk, F.J.; Levizzani, V.; Kirschbaum, D.; Tapiador, F.J.; Loew, A.; Borsche, M. Precipitation from space: Advancing Earth system science. *Bull. Am. Meteorol. Soc.* **2013**, *94*, 365–375. [CrossRef]
13. Hou, A.Y.; Kakar, R.K.; Neeck, S.; Azarbarzin, A.A.; Kummerow, C.D.; Kojima, M.; Oki, R.; Nakamura, K.; Iguchi, T. The Global Precipitation Measurements Mission. *Bull. Am. Meteorol. Soc.* **2014**, *95*, 701–722. [CrossRef]
14. Skofronick-Jackson, G.; Petersen, W.A.; Berg, W.; Kidd, C.; Stocker, E.F.; Kirschbaum, D.B.; Kakar, R.; Braun, S.A.; Huffman, G.J.; Iguchi, T.; et al. The Global Precipitation Measurement (GPM) Mission for Science and Society. *Bull. Am. Meteorol. Soc.* **2017**, *98*, 1679–1695. [CrossRef]
15. Lovejoy, S.; Schertzer, D.; Ladoy, P. Fractal characterization of inhomogeneous geophysical measuring networks. *Nature* **1986**, *319*, 43–44. [CrossRef]
16. Deidda, R.; Mascaro, G.; Piga, E.; Querzoli, G. An automatic system for rainfall signal recognition from tipping bucket gage strip charts. *J. Hydrol.* **2007**, *333*, 400–412. [CrossRef]

17. Hershfield, D.M.; Wilson, W.T. Generalizing of Rainfall-Intensity-Frequency Data. In *IUGG/IAHS Publication No. 43*; 1958; pp. 499–506. Available online: http://hydrologie.org/redbooks/a043/043051.pdf (accessed on 2 November 2020).

18. Hershfield, D.M. Rainfall frequency atlas of the United States for durations from 30 minutes to 24 hours and return periods from 1 to 100 years. In *US Weather Bureau Technical Paper N. 40*; U.S. Department of Commerce: Washington, DC, USA, 1961.

19. Weiss, L.L. Ratio of true to fixed-interval maximum rainfall. *J. Hydraul. Div.* **1964**, *90*, 77–82. [CrossRef]

20. Harihara, P.S.; Tripathi, N. Relationship of the clock-hour to 60-min and the observational day to 1440-min rainfall. *Ind. J. Meteorol. Geophys.* **1973**, *24*, 279–282. [CrossRef]

21. Natural Environment Research Council. *Flood Studies Report*; Natural Environment Research Council: London, UK, 1975.

22. Van Montfort, M.A.J. Sliding maxima. *J. Hydrol.* **1990**, *118*, 77–85. [CrossRef]

23. Faiers, G.E.; Grymes, J.M.; Keim, B.D.; Muller, R.A. A re-examination of extreme 24 hour rainfall in Louisiana, USA. *Clim. Res.* **1994**, *4*, 25–31. [CrossRef]

24. Van Montfort, M.A.J. Concomitants of the Hershfield factor. *J. Hydrol.* **1997**, *194*, 357–365. [CrossRef]

25. Young, C.B.; McEnroe, B.M. Sampling adjustment factors for rainfall recorded at fixed time intervals. *J. Hydrol. Eng.* **2003**, *8*, 294–296. [CrossRef]

26. Yoo, C.; Park, M.; Kim, H.J.; Choi, J.; Sin, J.; Jun, C. Classification and evaluation of the documentary-recorded storm events in the Annals of the Choson Dynasty (1392–1910), Korea. *J. Hydrol.* **2015**, *520*, 387–396. [CrossRef]

27. Papalexiou, S.M.; Dialynas, Y.G.; Grimaldi, S. Hershfield factor revisited: Correcting annual maximum precipitation. *J. Hydrol.* **2016**, *524*, 884–895. [CrossRef]

28. Morbidelli, R.; Saltalippi, C.; Flammini, A.; Cifrodelli, M.; Picciafuoco, T.; Corradini, C.; Casas-Castillo, M.C.; Fowler, H.J.; Wilkinson, S.M. Effect of temporal aggregation on the estimate of annual maximum rainfall depths for the design of hydraulic infrastructure systems. *J. Hydrol.* **2017**, *554*, 710–720. [CrossRef]

29. Morbidelli, R.; Saltalippi, C.; Flammini, A.; Corradini, C.; Wilkinson, S.M.; Fowler, H.J. Influence of temporal data aggregation on trend estimation for intense rainfall. *Adv. Water Resour.* **2018**, *122*, 304–316. [CrossRef]

30. Sevruk, B.; Klemm, S. Catalogue of national standard precipitation gauges. Instruments and observing methods. In *Report No. 39, WMO/TD-No. 313*; 1989. Available online: https://library.wmo.int/index.php?lvl=notice_display&id=11246#.YG179a8zZPY (accessed on 2 November 2020).

31. New, M.; Todd, M.; Hulme, M.; Jones, P.D. Precipitation measurements and trends in the twentieth century. *Int. J. Climatol.* **2001**, *21*, 1899–1922. [CrossRef]

32. Strangeways, I. *Precipitation: Theory, Measurement and Distribution*; Cambridge University Press: Cambridge, UK, 2007; ISBN 13978-0-521-85117-6.

33. Kidd, C.; Becker, A.; Huffman, G.J.; Muller, C.L.; Joe, P.; Skofronick-Jackson, G.; Kirschbaum, D.B. So, how much of the Earth's surface is covered by rain gauges? *Bull. Am. Meteorol. Soc.* **2017**, *98*, 69–78. [CrossRef]

34. Sun, Q.; Miao, C.; Duan, Q.; Ashouri, H.; Sorooshian, S.; Hsu, K.-L. A review of global precipitation data sets: Data sources, estimation, and intercomparisons. *Rev. Geophys.* **2018**, *56*, 79–107. [CrossRef]

35. Morbidelli, R.; García-Marín, A.P.; Al Mamun, A.; Atiqur, R.M.; Ayuso-Muñoz, J.L.; Bachir Taouti, M.; Baranowski, P.; Bellocchi, G.; Sangüesa-Pool, C.; Bennett, B.; et al. The history of rainfall data time-resolution in different geographical areas of the world. *J. Hydrol.* **2020**, *590*, 125258. [CrossRef]

36. Miller, J.F.; Frederick, R.H.; Tracey, R.J. *Precipitation-Frequency Atlas of the Western United States*; NOAA Atlas 2; National Weather Service, National Oceanic and Atmospheric Administration, U.S. department of Commerce: Washington, DC, USA, 1973.

37. Burlando, P.; Rosso, R. Scaling and multiscaling models of depth-duration-frequency curves for storm precipitation. *J. Hydrol.* **1996**, *187*, 45–64. [CrossRef]

38. Boni, G.; Parodi, A.; Rudari, R. Extreme rainfall events: Learning from raingauge time series. *J. Hydrol.* **2006**, *327*, 304–314. [CrossRef]

39. Balme, M.; Vischel, T.; Lebel, T.; Peugeot, C.; Galle, S. Assessing the water balance in the Sahel: Impact of small scale rainfall variability on runoff, Part 1: Rainfall variability analysis. *J. Hydrol.* **2006**, *331*, 336–348. [CrossRef]

40. Al-Rawas, G.A.; Valeo, C. Characteristics of rainstorm temporal distributions in arid mountainous and coastal regions. *J. Hydrol.* **2009**, *376*, 318–326. [CrossRef]

41. Coutinho, J.V.; Almeida, C.D.N.; Leal, A.M.F.; Barbosa, L.R. Characterization of sub-daily rainfall properties in three rainfall gauges located in Northeast of Brazil. Evolving Water Resources Systems: Understanding, Predicting and Managing Water-Society Interactions. *Proc. Int. Assoc. Hydrol. Sci.* **2014**, *364*, 345–350. [CrossRef]

42. Morbidelli, R.; Saltalippi, C.; Flammini, A.; Picciafuoco, T.; Dari, J.; Corradini, C. Characteristics of the underestimation error of annual maximum rainfall depth due to coarse temporal aggregation. *Atmosphere* **2018**, *9*, 303. [CrossRef]

43. Mann, H.B. Nonparametric tests against trend. *Econometrica* **1945**, *13*, 46–59. [CrossRef]

44. Kendall, M.G. *Rank Correlation Methods*; Griffin: London, UK, 1975.

45. Khaliq, M.N.; Ouarda, T.B.M.J.; Gachon, P.; Sushama, L.; St-Hilaire, A. Identification of hydrological trends in the presence of serial and cross correlation: A review of selected methods and their application to annual flow regimes of Canadian rivers. *J. Hydrol.* **2009**, *368*, 117–130. [CrossRef]

46. Sen, Z. Innovative trend analysis methodology. *J. Hydrol. Eng.* **2012**, *17*, 1042–1046. [CrossRef]

47. Willems, P. Adjustment of extreme rainfall statistics accounting for multidecadal climate oscillations. *J. Hydrol.* **2013**, *490*, 126–133. [CrossRef]

48. Alexandersson, H. A homogeneity test applied to precipitation data. *J. Climatol.* **1986**, *6*, 661–675. [CrossRef]

49. Pettitt, A.N. A non-parametric approach to the change-point detection. *Appl. Stat.* **1979**, *28*, 126–135. [CrossRef]